Int. J. Multiphase Flow, Vol. 5, pp. 281–291
Pergamon Elsevier, 1979. Printed in Great Britain

TRANSITION BOILING DATA OF WATER ON INCONEL SURFACE UNDER FORCED CONVECTIVE CONDITIONS

S. C. CHENG and H. RAGHEB
Department of Mechanical Engineering, University of Ottawa, Ottawa, Canada

(*Received* 8 *September* 1978; *in revised form* 10 *February* 1979)

Abstract—Transition boiling curves of distilled water on Inconel surfaces under forced convective conditions have been obtained. These data were generated from Inconel-copper composite test sections during quench experiments, using two-dimensional analysis. In order to properly account for axial conduction in the composite test sections, the two-dimensional model should be employed. An empirical correlation has been proposed, based on previous and present data.

1. INTRODUCTION

A high thermal capacity copper test section has been used recently to obtain boiling curves for distilled water at atmospheric conditions (Cheng *et al.* 1978a; Cheng *et al.* 1978c). The boiling curves were generated based on a 1-D model (one dimensional model) without considering axial conduction (Cheng & Heng 1976; Cheng *et al.* 1977a), since the axial conduction was found to be very small in the copper test section. For the purpose of studying the effect of heated surface thermal properties on boiling curves, composite test sections were constructed of a thin Inconel tubing soldered inside a thick copper cylindrical block. This arrangement is designed to maintain a long cooldown period in the transition boiling régime, thus permitting frequent and accurate temperature measurements. Since the thermal conductivity of Inconel is much lower than copper, it induces a larger axial temperature gradient, especially in the transition boiling régime, resulting in severe axial conduction during quench experiments. Thus, a 2-D analysis (Cheng 1978d; Cheng *et al.* 1978b) is necessary to properly account for the effect of axial conduction.

2. EXPERIMENTS

A typical composite test section, as shown in figure 1, consists of a 5.08 cm long cylindrical copper block with 9.53 cm outside diameter and a center bore of 1.296 cm allowing for the insertion of an Inconel tube. The Inconel tube with O.D. = 1.27 cm and thickness $\delta = 0.038$ cm is inserted into the copper block, with a gap of 0.013 cm between them provided for silver soldering. To ensure a uniform soldering, four strips of silver solder shim are inserted into the gap before soldering. A test section after soldering was cut into many pieces along the longitudinal direction, and it has been determined that the soldering layer is rather uniform without any visible voids.

The Inconel tube protudes from both ends of the test section for piping connections. Cartridge heaters are spaced around the test section and a total of six thermocouples are embedded. Five of them—located in the interface of the tube and silver solder—are to be used for data thermocouples (T.C. 2.2, T.C. 2.3 ... T.C. 2.6) as shown in figures 1 and 2. An extra thermocouple is embedded at 180° apart from T.C. 2.4 to check the circumferential effect on temperature measurements; it has been found that this effect is negligibly small. The test section is insulated by thick ceramic fiber insulation. Subcooled distilled water at atmospheric conditions is introduced from the bottom of the test section during quench experiments. Detailed experimental apparatus and procedures may be found in the work by Cheng *et al.* (1978c) and Cheng *et al.* (1977b).

3. EXPERIMENTAL RESULTS

A typical set of boiling curves for a mass flux of 136 kg/m^2 sec and an inlet subcooling of 13.9°C was constructed using the 2-D analysis (Cheng 1978d; Cheng *et al.* 1978b) as shown in

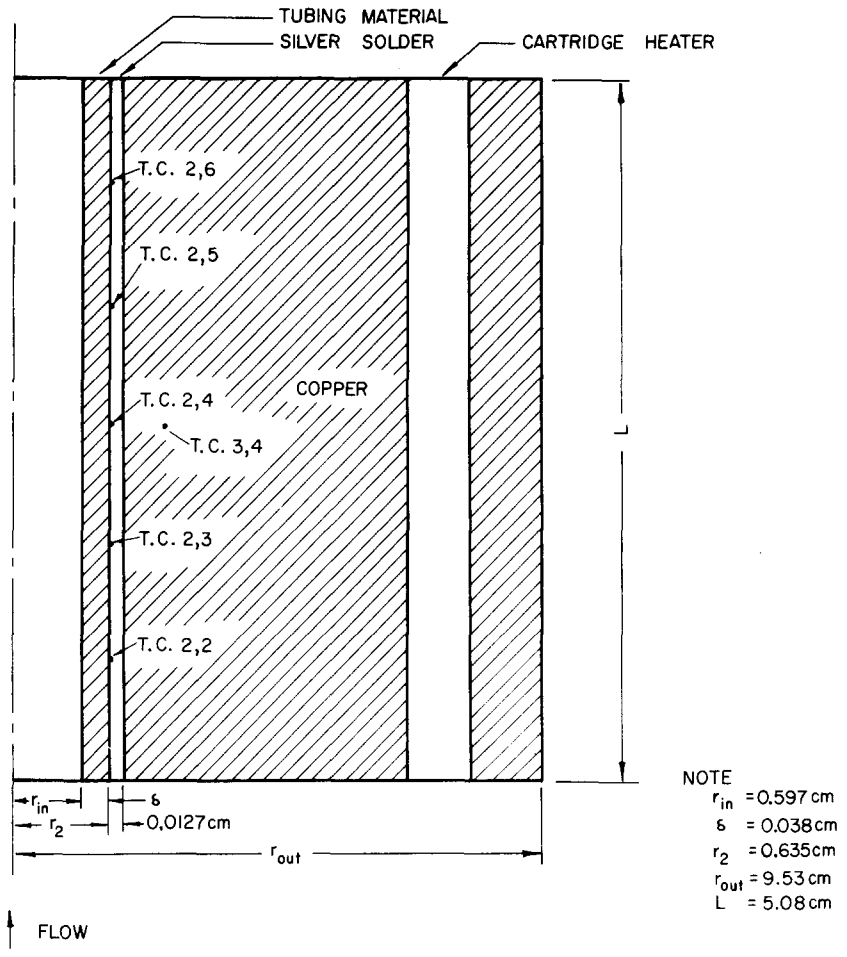

Figure 1. Locations of thermocouples in composite test sections.

figure 3, while figure 4 presents the corresponding 1-D results. Basically, the 2-D analysis allows one to calculate heat flux from a given section j (inside the test section), as shown in figure 2 through plane j to the fluid at time t, by computing the rate of change in heat content of that section, plus axial conduction from neighboring sections at the same time t. For simplicity, the test section has been assumed to be perfectly insulated in the analysis.

A large spread in boiling curves is noticed for the 2-D results. In order to gain some insight into the cause of the spread, the test section temperature distribution will be examined in detail. Figure 5 illustrates the axial data thermocouple temperature distributions as well as the inner wall temperature distributions. The following observations can be made:

(a) At $t = 100$ sec, the rewet front† has already gone through planes 2 and 3, while planes 4, 5 and 6 are still in the film boiling régime. A small thermocouple temperature gradient occurs between planes 5 and 6 reflecting a small amount of heat loss through the top end of the test section.

(b) Some typical temperature distributions in the transition boiling régime which occur at $t = 203$ sec, are shown in the figure. At this time, the rewet front has passed through plane 4.

(c) At $t = 211$ sec, CHF‡ occurs at planes 2 and 3 as evidenced by sharp temperature gradients and a large spread between the data thermocouple temperature and the corresponding inner wall temperature at each section.

(d) At $t = 216$ sec, CHF occurs at planes 4–6.

†The onset of rewet point in this paper is defined as the intersection point of the film boiling régime (which is almost a flat line based on this study) and the transition boiling régime (Ragheb *et al.* 1978).

‡CHF in this paper is referred to the maximum heat flux point of a boiling curve.

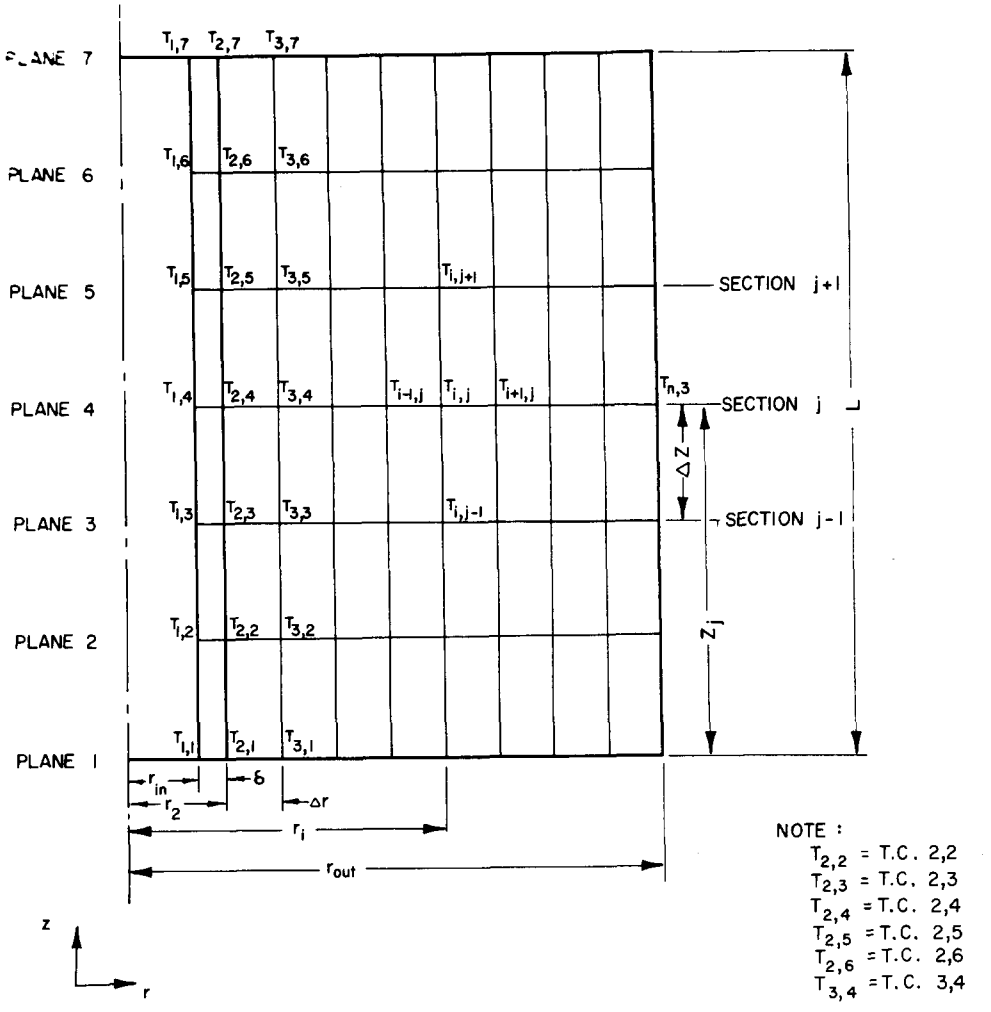

Figure 2. Nodal network for two dimensional model in composite test sections.

(e) Some typical temperature distributions in the nucleate boiling régime which occur at $t = 282$ sec, are shown. From the thermocouple temperature distribution, it clearly indicates some axial heat loss and possible end effects occurred at both ends of the test section.

Figures 6 and 7 illustrate the radial temperature distributions at $t = 100$, 211 and 282 sec. In general, steep temperature gradients exist near the inner wall surface (nodal point 1). At $t = 100$ and 282 sec, all five sectional radial temperature distributions are very similar except in the region close to the inner wall surface. At $t = 211$ sec, a large spread is observed among the five radial temperature distributions. This is because CHF occurs at planes 2 and 3 as evidenced by the existence of sharp temperature drops between nodal points 2 and 1 on both sections 2 and 3.

Boiling curves based on 2-D and 1-D analysis were generated for other mass flux and subcoolings (Cheng *et al.* 1978b). Based on their 1-D and present 1-D data, all evaluated at the mid-plane, a new empirical correlation for the Inconel surface is found as follows:

$$\phi = 0.820[5266.6(\Delta T_{sat})^{0.75} + 107910.0\Delta T_{sat} \exp(-0.025\Delta T_{sat})] \exp[(0.0045\Delta T_{sub} + 0.0005G) \ln \Delta T_{sat}]$$

where ϕ is the heat flux (W/m^2); ΔT_{sat} is the wall superheat (°C); G is the mass flux; 68–203 kg/m^2 sec; and ΔT_{sub} is the inlet subcooling of the liquid; 0–27.8°C. The form of the empirical correlation is similar to Hsu's expression (1974), but has been modified by

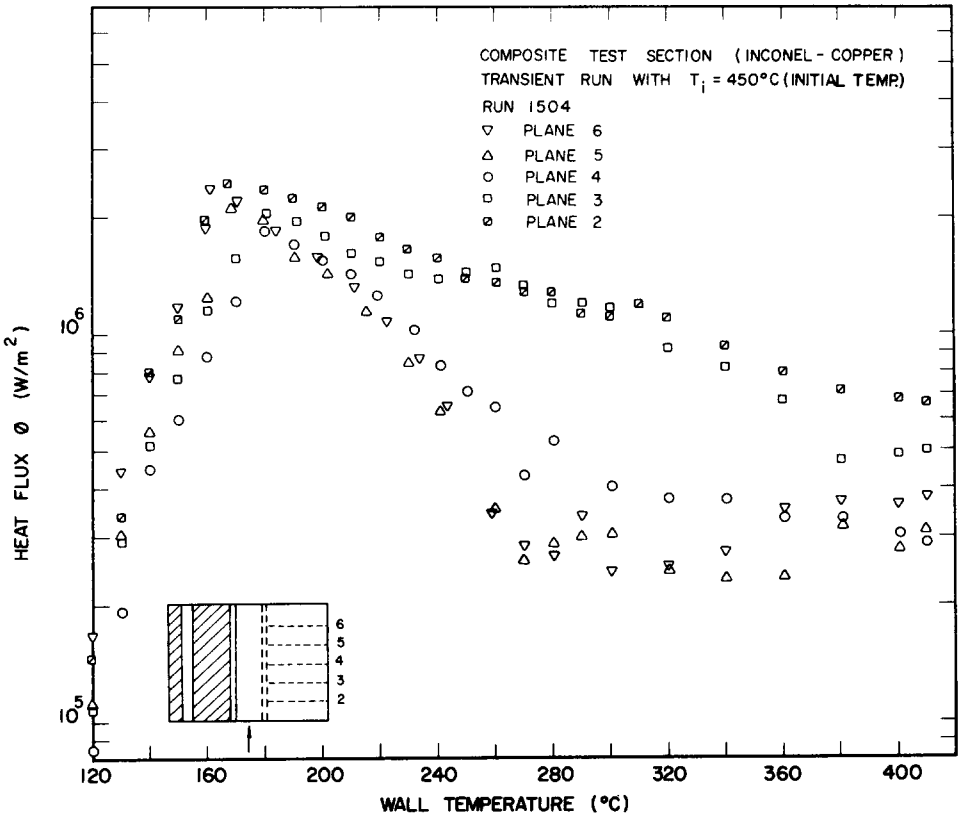

Figure 3. Boiling curves of distilled water for $G = 136\ \text{kg/m}^2\ \text{sec}$ and $\Delta T_{sub} = 13.9°\text{C}$, using 2-D model.

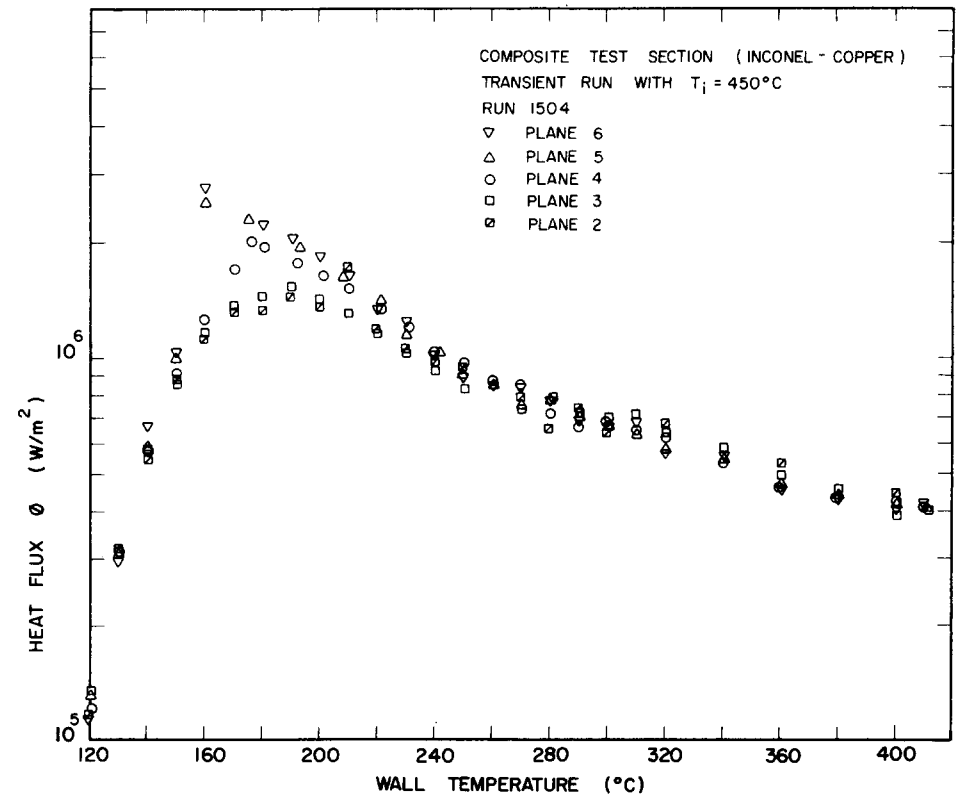

Figure 4. Boiling curves of distilled water for $G = 136\ \text{kg/m}^2\ \text{sec}$ and $\Delta T_{sub} = 13.9°\text{C}$, using 1-D model.

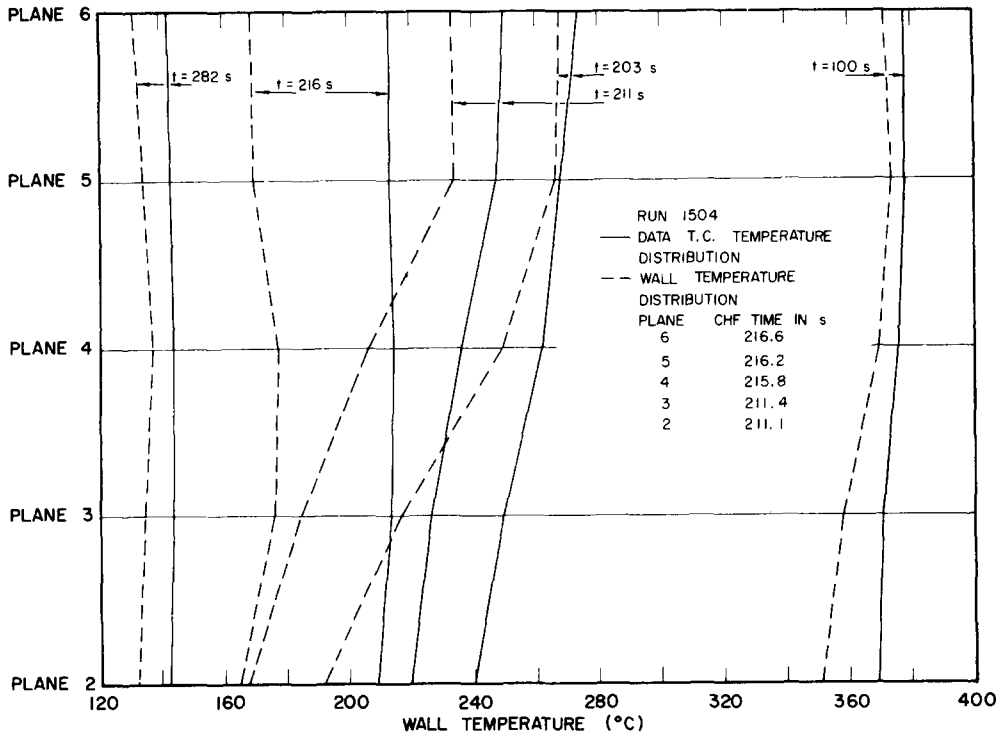

Figure 5. Axial temperature distributions for $G = 136\ \text{kg/m}^2\ \text{sec}$ and $\Delta T_{sub} = 13.9°\text{C}$, using 2-D model.

incorporating the effects of subcooling and mass flux. The correlation was obtained over 452 data points (from nine test runs) with an rms error of 9.7%.

The effect of subcooling on boiling curves at $G = 136\ \text{kg/m}^2\ \text{sec}$ is presented in figure 8, while the effect of mass flux at $\Delta T_{sub} = 13.9°\text{C}$, is shown in figure 9. Heat flux increases with increasing subcooling and mass flux; this indicates the same parametric trends as reported previously for the copper test section (Cheng *et al.* 1978a; Cheng *et al.* 1978c).

4. DISCUSSION

In general, the values of CHF and minimum heat flux generated by the Inconel-copper test section are about the same as those of copper test section. A typical comparison is illustrated in figure 10. However, the rewetting for the composite test section is found to be at approx. 100–150°C higher wall temperature and CHF 30°C higher wall temperature. This is in agreement with the findings of Henry (1974) and Yao & Henry (1978). They found that for a lower value of $k\rho c_p$ (such as Inconel surface in this study), a higher minimum film boiling temperature is required to sustain stable film boiling. Here, the value of the minimum film boiling temperature is assumed to be very close to the rewet temperature.

Concerning the 2-D analysis, it should be pointed out that the model is very sensitive to (a) the soldering of test section and thermocouples, (b) the exact locations of thermocouples and (c) the accuracy of each data thermocouple measurement. The contact resistance between the tube and the copper block may have some effect on the resulting boiling curves. However, preliminary analysis based on the existing set-up indicates that its effect is very small.

For simplicity, heat losses are not incorporated in the 2-D model. It is assumed that heat losses from the test section through the tube to the connection piping and from the test section through the insulation to the surroundings, are small. The former is justified by the use of very thin tubing with a low value of thermal conductivity.

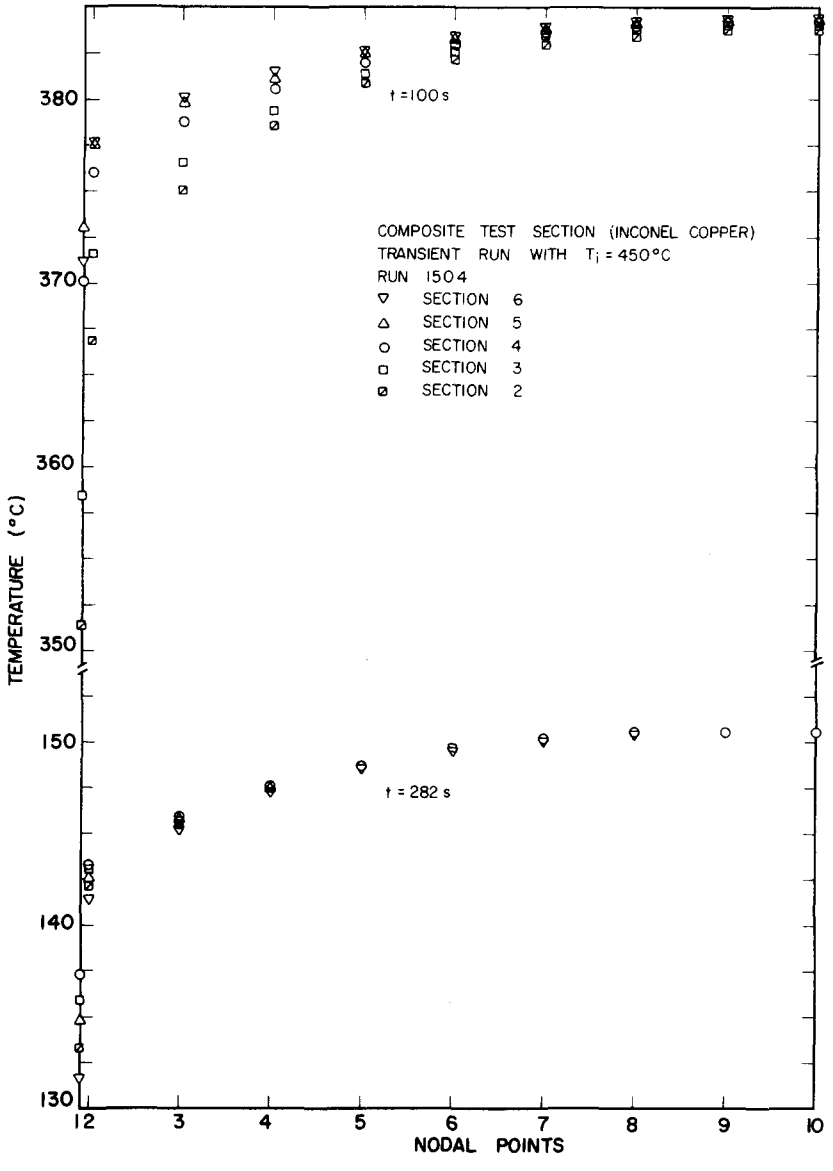

Figure 6. Radial temperature distributions for $G = 136\ kg/m^2\ sec$ and $\Delta T_{sub} = 13.9°C$, using 2-D model (part I).

The plane 6 boiling curve in the film boiling régime is always higher than plane 5 boiling curve and an example is shown in figure 3. This is possibly due to (a) neglecting axial heat losses and (b) end effects resulting in more efficient heat transfer. Also, the plane 2 boiling curve in film and transition boiling régimes, in general, is found to be noticeably higher than other boiling curves regardless of the inlet subcooling and mass flux. This is attributed to (a) the lowest bulk fluid temperature, (b) entrance and end effects and (c) neglecting axial heat losses. In the transition boiling régime, all the five boiling curves show a correct trend against the bulk fluid temperature. The heat losses in this régime should be negligibly small in comparison with a rather high level of axial conduction taking place inside the test section.

In the nucleate boiling régime, planes 2 and 6 boiling curves are higher than others, this is due to the same reasons as explained in the film boiling case.

It has been found in the studies of copper test section that, (a) the mid-plane boiling curve based on 2-D analysis represents the average boiling curve for the entire test section, and a

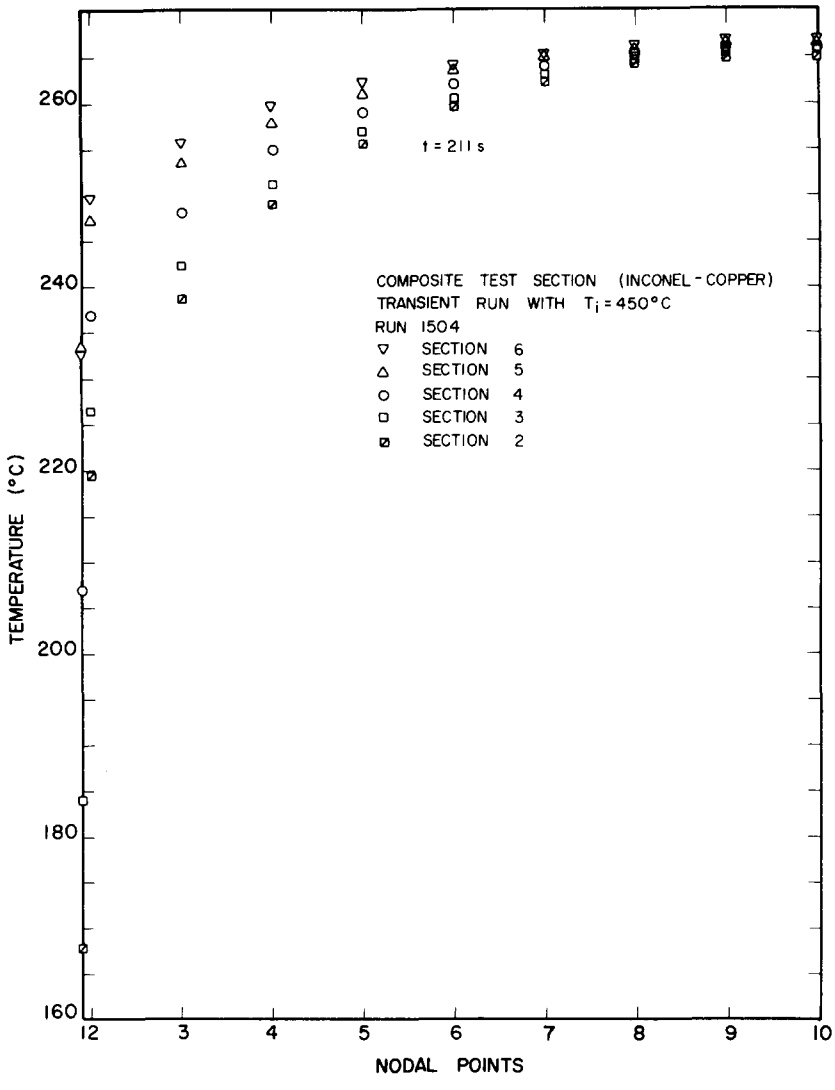

Figure 7. Radial temperature distributions for $G = 136$ kg/m^2 sec and $\Delta T_{sub} = 13.9$°C, using 2-D model (part II).

similar observation can again be made for 1-D analysis, (b) the two mid-plane boiling curves based on 2-D and 1-D models, respectively, are approximately the same and (c) the net axial conduction gain at the mid-section, based on 2-D analysis is very small and for practical purposes, it can be assumed to be zero. In the present study, the plane 4 (mid-plane) boiling curve of 1-D model (figure 4) falls somewhere between the plane 3 and plane 4 boiling curves for the corresponding 2-D model (figure 3). This suggests that the zero axial conduction section has been shifted down from the mid-section as evidenced from axial temperature distributions in figure 5.

Some steady state results are obtained as shown in figure 11, good agreement is observed with transient data evaluated at mid-plane, using 1-D analysis. This is anticipated as both sets of data representing the average boiling curve for the test section. During steady state operation, the heat flux to the fluid was measured directly from the power input to the heaters (Cheng *et al.* 1978c; Cheng *et al.* 1977b).

For the purpose of studying the effect of thermal properties on boiling curves, other composite test sections such as stainless steel–copper and Zircaloy-copper are under investigation at the present time.

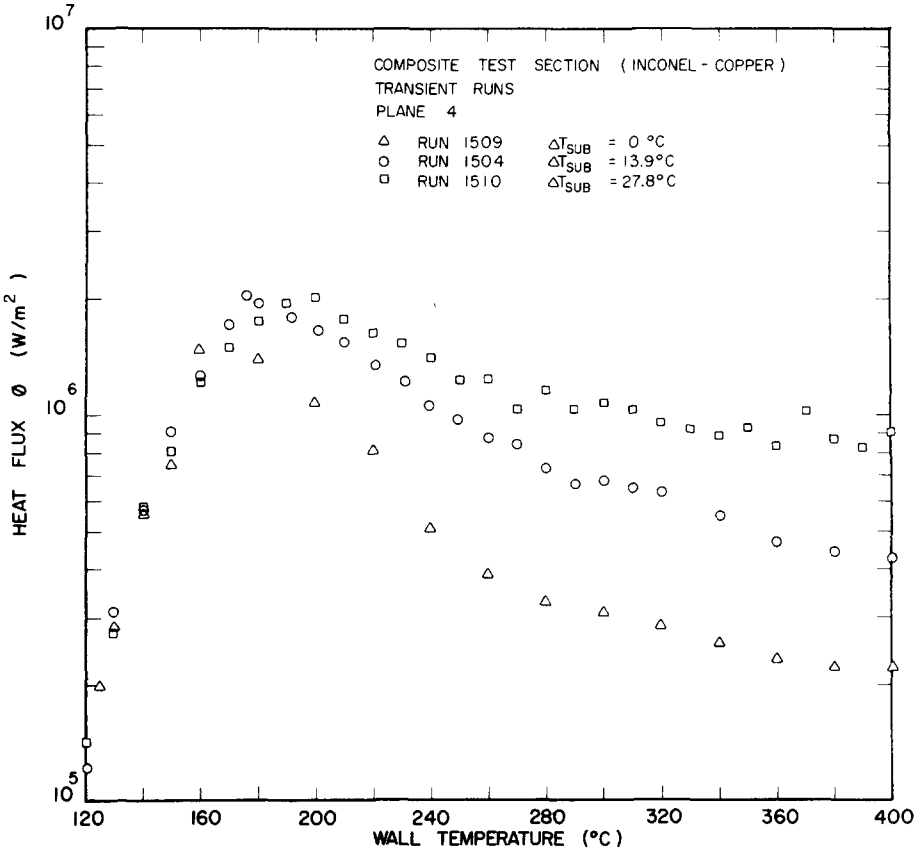

Figure 8. Effect of subcooling on boiling curves of distilled water for $G = 136\ \text{kg/m}^2\,\text{sec}$, using 1-D model.

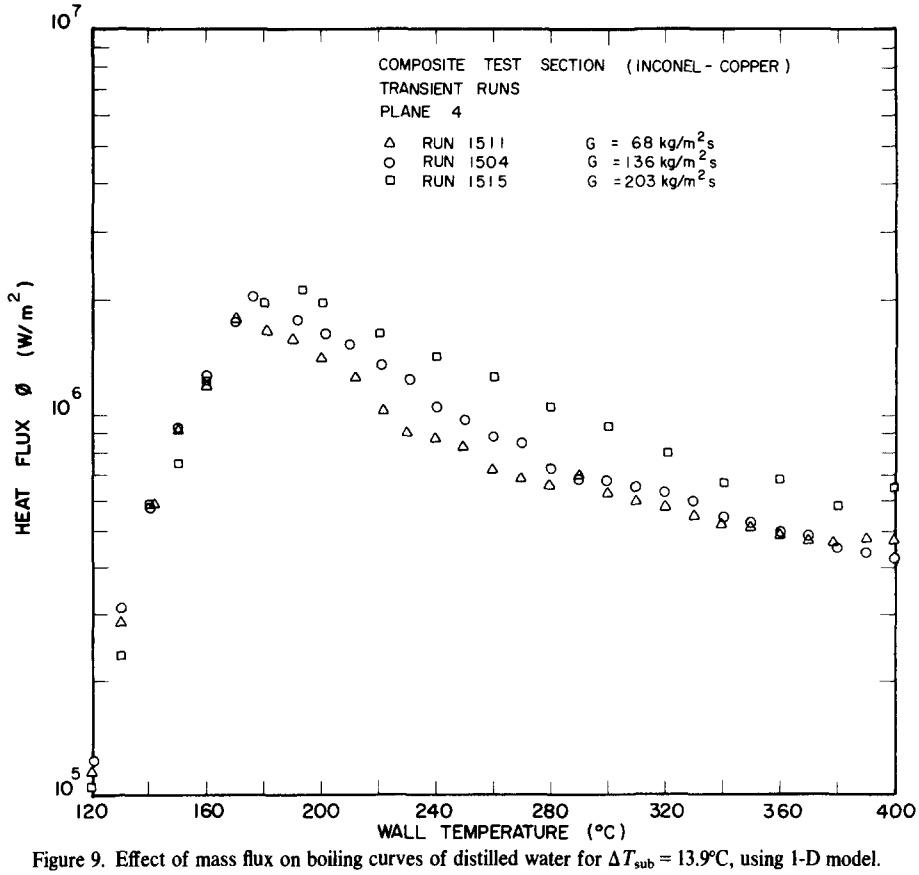

Figure 9. Effect of mass flux on boiling curves of distilled water for $\Delta T_{sub} = 13.9°C$, using 1-D model.

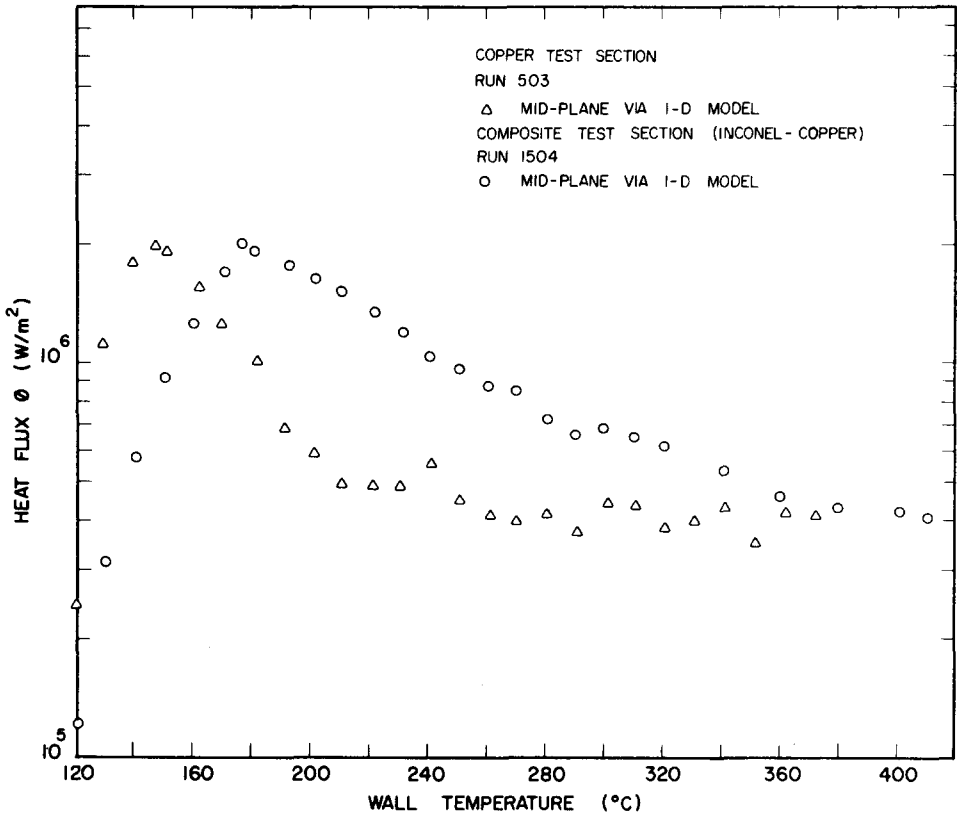

Figure 10. Comparison of boiling curves for copper test section and Inconel-copper test section at $G = 136\ \text{kg/m}^2\ \text{sec}$ and $\Delta T_{sub} = 13.9°\text{C}$.

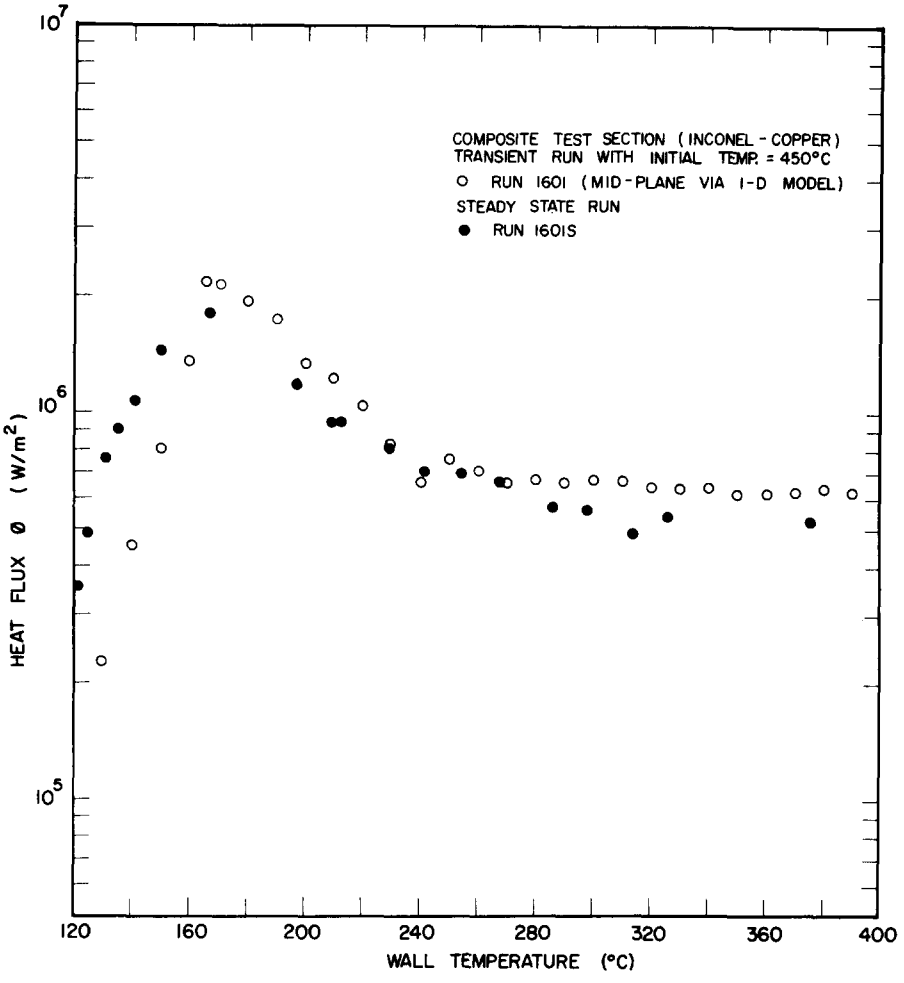

Figure 11. Boiling curves of distilled water for $G = 136\ \text{kg/m}^2\,\text{sec}$ and $\Delta T_{sub} = 13.9°\text{C}$, using transient and steady state methods.

5. CONCLUSIONS

(1) Transition boiling curves obtained via both 1-D and 2-D models have been investigated. The large spread in boiling curves via 2-D analysis was discussed. The boiling curve generated via 1-D model evaluated at mid-plane represents the average heat flux for the test section and this is in agreement with steady state data.

(2) To generate local transition boiling curves on an Inconel surface, the 2-D model must be employed in order to properly account for axial conduction.

Acknowledgements—The authors wish to express their gratitude to the U.S. Nuclear Regulatory Commission and the National Research Council of Canada for providing the financial support for this project.

REFERENCES

CHENG, S. C. 1978d Transition boiling curves generated from quenching experiments using a two-dimensional model. *Lett. Heat Mass Trans.* **5**, 391–403.

CHENG, S. C. & HENG, K. T. 1976 A technique to construct a boiling curve from quenching data. *Lett. Heat Mass Trans.* **3**, 413–420.

CHENG, S. C., HENG, K. T. & NG, W. W. L. 1977a A technique to construct a boiling curve from quenching data considering heat loss. *Int. J. Multiphase Flow* **3**, 495–499.

CHENG, S. C., NG, W. W. L. & HENG, K. T. 1978c Measurements of boiling curves of subcooled water under forced convective conditions. *Int. J. Heat & Mass Trans.* **21**, 1385–1392.

CHENG, S. C., NG, W. W. L., HENG, K. T. & GROENEVELD, D. C. 1978a Measurements of transition boiling data for water under forced convective conditions. *J. Heat Trans.* **100**, 382–384.

CHENG, S. C., NG, W. W. L., HENG, K. T. & RAGHEB, H. 1977b Transition boiling heat transfer in forced vertical flow. Final Report, for the period June 1976–June 1977, Argonne Contract 31-109-38-3564.

CHENG, S. C., RAGHEB, H., NG, W. W. L., HENG, K. T. & ROY, S. 1978b Transition boiling heat transfer in forced vertical flow. Final Report, for the period June 1977–June 1978, NUREG/CR-0357 and ANL-78-75.

HENRY, R. E. 1974 A correlation for the minimum film boiling temperature. *A.I.Ch.E. Symp. Series No.* 138, 70, 81–90.

HSU, Y. Y. 1974 Tentative correlation of reflood heat transfer. Presented at the 3rd Water Reactor Safety Information Meeting, Germantown, MD.

RAGHEB, H. S., CHENG, S. C. & GROENEVELD, D. C. 1978 Measurement of transition boiling boundaries in forced convective flow. *Int. J. Heat & Mass Trans.* **21**, 1621–1624.

YAO, S. C. & HENRY, R. E. 1978 An investigation of the minimum film boiling temperature on horizontal surfaces. *J. Heat Trans.* **100**, 260–267.